

AT 675316

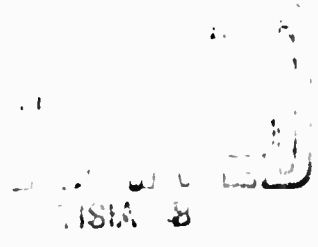
ANALYTIC EVALUATION OF THE FOURIER COEFFICIENTS
OF A CLIPPED PERIODIC FUNCTION

Marvin Blum

| COPY | OF | Price |
|------------|----|---------|
| HARD COPY | 2 | \$.200 |
| MICROFICHE | 3 | \$.500 |

415

May 1965

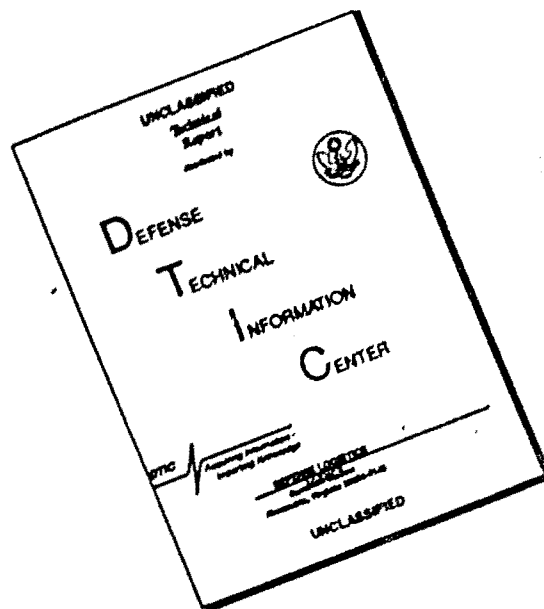


P-3137

Approved for OIS release

ARCHIVE COPY

DISCLAIMER NOTICE



THIS DOCUMENT IS BEST QUALITY AVAILABLE. THE COPY FURNISHED TO DTIC CONTAINED A SIGNIFICANT NUMBER OF PAGES WHICH DO NOT REPRODUCE LEGIBLY.

ANALYTIC EVALUATION OF THE FOURIER COEFFICIENTS
OF A CLIPPED PERIODIC FUNCTION

Marvin Blum^{*}

The RAND Corporation, Santa Monica, California

ABSTRACT

For periodic input $u(t)$, a time representation $c(t)$ for the clipper is obtained such that the output $y(t) = c(t) u(t)$. The Fourier coefficients of $y(t)$ are obtained in terms of the Fourier coefficients of both $c(t)$ and $u(t)$. For light clipping, the Fourier coefficients of $y(t)$ equal the Fourier coefficients of $u(t)$ plus a small correction factor of the order of the percent of time the signal exceeds clipping limits. An exact expression for the correction factor is obtained which may require numerical solutions. Some algorithms for obtaining numerical solutions are discussed.

^{*} Any views expressed in this paper are those of the author. They should not be interpreted as reflecting the views of The RAND Corporation or the official opinion or policy of any of its governmental or private research sponsors. Papers are reproduced by The RAND Corporation as a courtesy to members of its staff.

ACKNOWLEDGMENT

The author would like to express his gratitude to Dr. E. Bedrosian of The RAND Corporation for his assistance in motivating this study, as well as for his assistance in the presentation of the results of the study.

CONTENTS

| | |
|--|----|
| ABSTRACT..... | 1 |
| ACKNOWLEDGEMENT..... | 2 |
| LIST OF FIGURES..... | 4 |
| Section | |
| I. INTRODUCTION..... | 5 |
| II. TIME FUNCTION REPRESENTATION OF A CLIPPING FUNCTION..... | 7 |
| III. FOURIER SERIES REPRESENTATION..... | 9 |
| Fourier Series Expansion of Clipping Function..... | 10 |
| General Properties of the Limiter Fourier Coefficients..... | 11 |
| Convergence of Correction Series..... | 13 |
| Appendix | |
| A. NARROW SINGLE SIDE-BAND TRANSMISSION..... | 17 |
| B. BROAD-BAND SIGNALS..... | 32 |
| C. SENSITIVITY OF THE VALUE OF INTEGRALS $I_j(m)$ TO CARRIER FREQUENCY ω_c | 37 |
| REFERENCES..... | 40 |

LIST OF FIGURES

| | |
|--|----|
| 1. Ideal clipper characteristics | 7 |
| 2. Typical signal $u(t)$ versus t with occasional spikes | 12 |
| 3. Typical curve of $f(t)$ and its time derivative $f'(t)$ | 14 |
| 4. Band-limited signals | 17 |
| 5. Magnitude of Fourier coefficients versus frequency for (a) modulation signal; (b) carrier signal; (c) frequency translated signal, double side bands; and (d) frequency translated signal, single side band | 19 |
| 6. Modulation signal $s(t)$ superimposed on harmonic carrier | 21 |
| 7. Typical display of clipped peaks of transmitted signal for $t \in R_1$ and R_2 showing fine structure of carrier function | 28 |
| 8. Analog solution for the Fourier coefficients d_m of the limit function $c(t)$ | 33 |
| 9. Analog solution for times $t \in R_1 \cup R_2$ | 35 |

I. INTRODUCTION

A single side-band amplitude modulated signal has the desirable property of requiring a transmission bandwidth no greater than that of the modulating or information signal. However, the modulated signal may contain signal peaks which were not present in the modulation signal. These induced peaks can increase the ratio of peak to average signal power, thereby imposing more severe demands of linearity on the transmitter.

In practice, single side-band amplitude modulated signals occasionally exceed the linear range either inadvertently or deliberately if a certain amount of distortion can be tolerated. To assess the magnitude of this distortion, this paper considers an asymmetrical clipping, where the modulated signal is unchanged between levels K_2 and K_1 and clipped at $K_2 > 0$, $K_1 < 0$. In general, since it is desirable to transmit the modulated signal without excessive distortion, the degree of clipping must be small.

Clipping as an example of nonlinear processing has been discussed extensively in the literature.^(1,2) Clipping reduces the peak factor of the modulated signal and increases the bandwidth of the signal. The original modulated signal bandwidth must be restored by filtering.

Previous analytic treatment of the effects⁽¹⁾ of the clipper considered the action of the clipper in the form

$$y(t) = P(u(t))$$

where $y(t)$ is the output and P is the nonlinear transformation on the input signal $u(t)$. The nonlinear transformation is approximated by

$$P(u(t)) = \sum_{k=0}^m \alpha_k [u(t)]^k$$

e.g., a polynomial expansion of the input where m is chosen so a sufficiently good approximation is obtained. This leads to extremely cumbersome computational requirements for even moderately small m .

In this paper, $u(t)$ is restricted to periodic signals,^{*} and a time representation $c(t)$ for the clipper is obtained such that

$$y(t) = c(t)u(t)$$

The Fourier coefficients of $y(t)$ are obtained in terms of the Fourier coefficients of both $c(t)$ and $u(t)$. It is shown that for light clipping, the Fourier coefficients of $y(t)$ equal the Fourier coefficients of $u(t)$ plus a small correction of the order of the per cent of the time the signal $u(t)$ exceeds the clipping limits. It is believed that the computations required to obtain these corrections are greatly simplified as compared to existing analytical techniques. Very accurate estimates of the Fourier coefficients are obtainable without requiring intractable high-order expansion.

*The Fourier coefficients of the assumed periodic signal $y(t)$ can be approximations to the Fourier transform of $u(t)$ if $u(t)$ is not strictly periodic.

II. TIME FUNCTION REPRESENTATION OF A CLIPPING FUNCTION

Let $u(t)$ be the input to a clipper and $y(t)$ the output signal. It is assumed that $u(t)$ is periodic with period $T = 1/f_0$. The clipper characteristics are shown in Fig. 1.

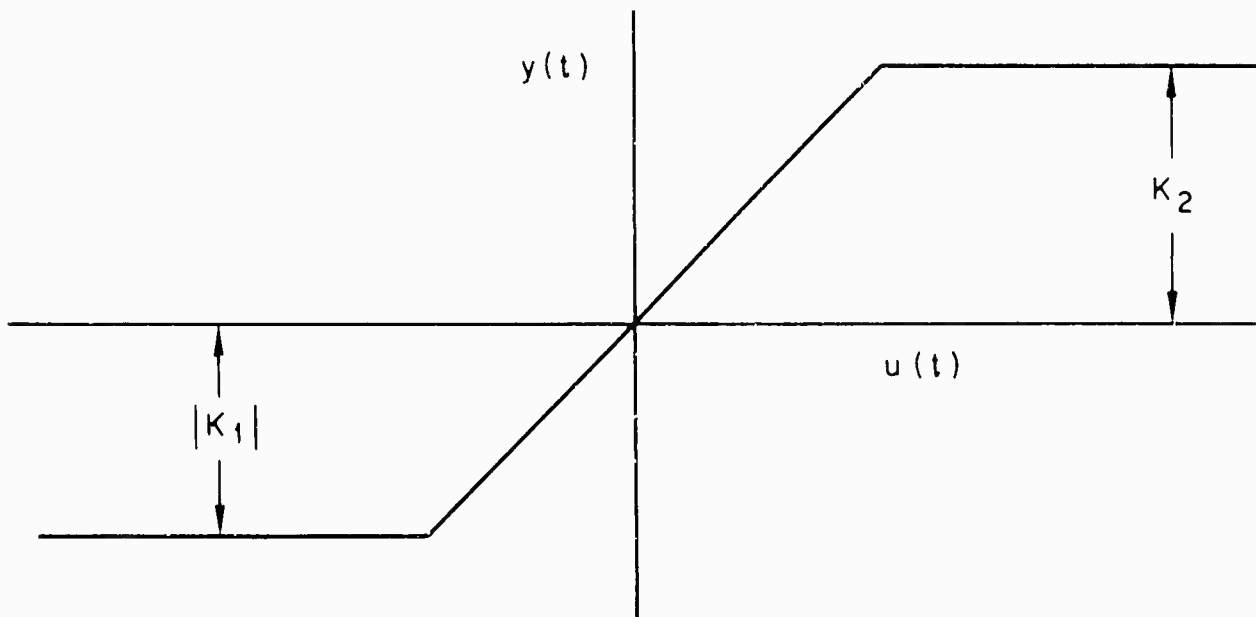


Fig.1—Ideal clipper characteristics

That is

$$\begin{aligned}
 y(t) &= u(t), & K_1 \leq u(t) \leq K_2 \\
 &= K_1, & \text{when } u(t) < K_1, & K_1 < 0 \\
 &= K_2, & \text{when } u(t) > K_2, & K_2 > 0
 \end{aligned} \tag{1}$$

Regions can be defined on the time axis R_j such that

$$\begin{aligned}
 t \in R_2 \quad u(t) > K_2 \\
 t \in R_1 \quad u(t) < K_1 \\
 t \in R_0 \quad K_1 \leq u(t) \leq K_2
 \end{aligned} \tag{2}$$

The clipper action can be characterized by the following time function

$$y(t) = u(t) \cdot c(t) \tag{3}$$

where

$$c(t) = 1, \quad t \in R_0$$

$$c(t) = \frac{K_1}{u(t)}, \quad t \in R_1 \tag{4}$$

$$c(t) = K_2/u(t) \quad t \in R_2$$

It is seen that $u(t)$ periodic with period T implies that $c(t)$ is also periodic with period T .

III. FOURIER SERIES REPRESENTATION

Assuming that $u(t)$ has a Fourier series representation

$$u(t) = \sum_{n=-\infty}^{+\infty} c_n e^{in\omega_0 t} \quad (5)$$

where

$$c_n = \frac{1}{T} \int_{\tau}^{\tau+T} u(t) e^{-in\omega_0 t} dt, \quad \omega_0 = 2\pi/T$$

Since $c(t)$ is periodic with period T , a Fourier series expansion exists as $0 \leq c(t) \leq 1$, and the Fourier series expansion of $u(t)$ has been assumed to exist. Then $c(t)$ may be written as

$$c(t) = \sum_{m=-\infty}^{+\infty} d_m e^{im\omega_0 t} \quad (6)$$

An evaluation of the d_m is presented later in this section.

By Eq. (3), the output $y(t)$ is the product of two periodic functions (each of period T). The output is therefore periodic with period T and has a Fourier series representation of the form of Eq. (5). Then

$$y(t) = \sum_{l=-\infty}^{+\infty} f_l e^{il\omega_0 t} \quad (7)$$

where

$$f_l = \frac{1}{T} \int_{\tau}^{\tau+T} y(t) e^{-il\omega_0 t} dt \quad (8)$$

The coefficients f_ℓ can be represented by the convolution of the coefficients c_m and d_m as follows

$$f_\ell = \frac{1}{T} \int_{\tau}^{\tau+T} \sum_{n=-\infty}^{+\infty} \sum_{m=-\infty}^{+\infty} d_n d_m e^{i(n+m-\ell)\omega_0 t} dt \quad (9)$$

The integral

$$\frac{1}{T} \int_{\tau}^{\tau+T} e^{iu\omega_0 t} dt = \delta_{0,u}, \quad u = 0 \pm 1, \pm 2, \dots \quad (10)$$

where

$$\begin{aligned} \delta_{ij} &= 1, \quad i = j \\ \delta_{ij} &= 0, \quad i \neq j \end{aligned} \quad (11)$$

Therefore

$$f_\ell = \sum_{n=-\infty}^{+\infty} c_n d_{\ell-n} = \sum_{m=-\infty}^{+\infty} c_{\ell-m} d_m \quad (12)$$

The coefficients c_m are known, since the input function $u(t)$ is known. It now is required to evaluate the coefficients d_m of the clipping function $c(t)$.

FOURIER SERIES EXPANSION OF CLIPPING FUNCTION

Using the inversion relationship shown in Eq. (5)

$$\begin{aligned} d_m &= \frac{1}{T} \int_{\tau}^{\tau+T} c(t) e^{-im\omega_0 t} dt \\ &= \frac{1}{T} \int_{t \in R_0} e^{-im\omega_0 t} dt + \int_{t \in R_1} \frac{K_1}{u(t)} e^{-im\omega_0 t} dt + \int_{t \in R_2} \frac{K_2}{u(t)} e^{-im\omega_0 t} dt \end{aligned} \quad (13)$$

$$d_m = f_{m,0} + \frac{1}{T} \int_{t \in R_1} \frac{K_1 - u(t)}{u(t)} e^{-im\omega_0 t} dt + \frac{1}{T} \int_{t \in R_2} \frac{K_2 - u(t)}{u(t)} e^{-im\omega_0 t} dt \quad (14)$$

$$m = 0, \pm 1, \pm 2, \dots$$

GENERAL PROPERTIES OF THE LIMITER FOURIER COEFFICIENTS

Let

$$I_1(m) = \frac{1}{T} \int_{t \in R_1} \frac{K_1 - u(t)}{u(t)} e^{-im\omega_0 t} dt \quad (15)$$

$$I_2(m) = \frac{1}{T} \int_{t \in R_2} \frac{K_2 - u(t)}{u(t)} e^{-im\omega_0 t} dt \quad (16)$$

Note first that

$$0 \leq \frac{K_j - u(t)}{u(t)} < -1 \quad j = 1, 2 \quad (17)$$

so that

$$|I_j(m)| \leq L(R_j)/T \quad (18)$$

where $L(R_j)$ = length of the regions R_j .

Thus, if the limiting of $u(t)$ occurs over relatively few spikes of narrow width, as shown in Fig. 2, the change in the coefficients

$$|c_m - f_m| \approx 0 \left(\frac{L(R_1 \cup R_2)}{T} \right).$$

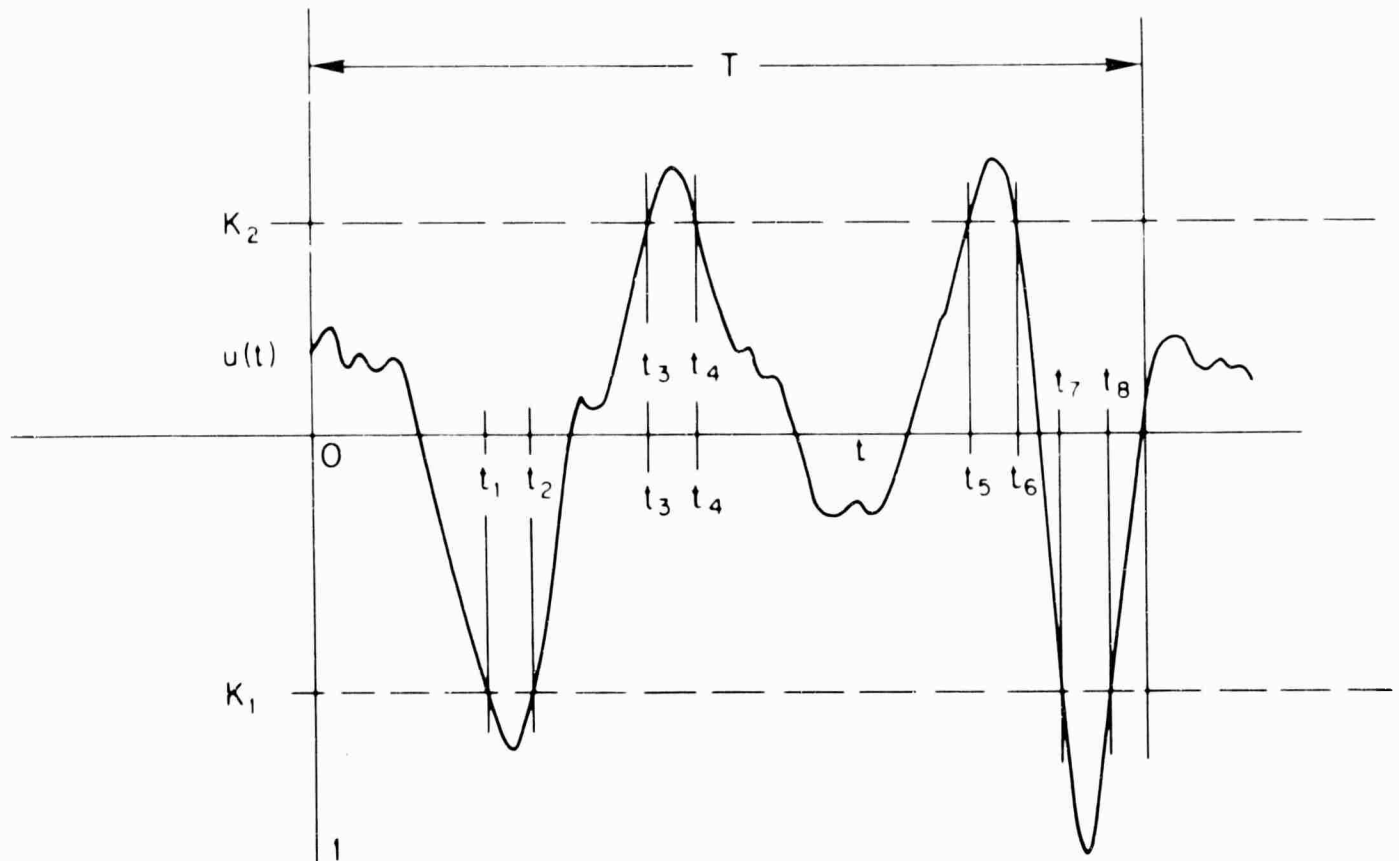


Fig.2—Typical signal $u(t)$ versus t with occasional spikes

From Eq. (16)

$$d_0 = 1 + I_1(0) + I_2(0) \quad (19)$$

where

$$|I_1(0)| = \frac{(t_2 - t_1) + (t_8 - t_7)}{T} \quad (20)$$

$$|I_2(0)| = \frac{(t_4 - t_3) + (t_6 - t_5)}{T}$$

Thus, I_1 and I_2 are small corrections to unity if the sum of the intervals $\ll T$. Let this condition be termed light limiting.

Similarly

$$d_m = [I_1(m) + I_2(m)] \quad m \neq 0 \quad (21)$$

$$d_m \approx 1 \quad \text{for light limiting.}$$

Thus, Eq. (12) may be written as

$$f_f = c_f + \sum_{n=-\infty}^{+\infty} c_n [I_1(f - n) + I_2(f - n)] \quad (22)$$

Equation (22) then shows that $f_f = c_f +$ small correction term under light limiting conditions.

CONVERGENCE OF CORRECTION SERIES

It will be shown that the coefficients d_m fall off as (m^{-2}) provided $u'(t)$ is bounded in R_1UR_2 so that the summation in Eq. (22) would not require too many terms to obtain accurate corrections to f_f .

Let

$$\begin{aligned} \Psi(t) &= 0, \quad t \in R_0 \\ &= \frac{K_1 - u(t)}{u(t)}, \quad t \in R_1 \\ &= \frac{K_2 - u(t)}{u(t)}, \quad t \in R_2 \end{aligned}$$

Then

$$d_m = \frac{1}{T} \int_{+\tau}^{T+\tau} \Psi(t) e^{-im\omega_0 t} \quad m \neq 0$$

A typical curve for $\Psi(t)$ and its derivative is shown in Fig. 3. The essential consideration is that $\Psi'(t)$ is bounded in the interval

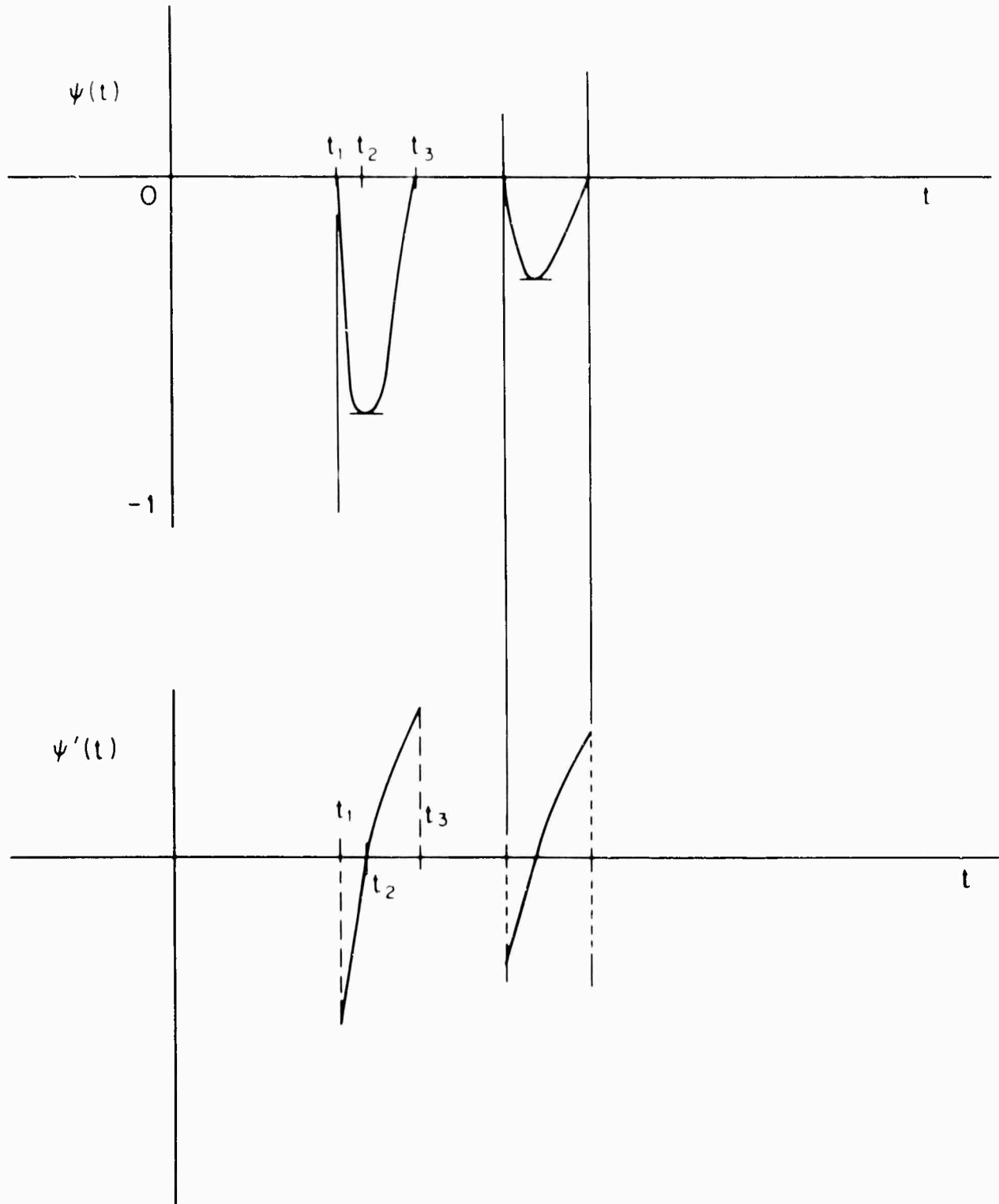


Fig. 3—Typical curve of $\psi(t)$ and its time derivative $\psi'(t)$

$\tau, \tau+T$ and has jump discontinuities at the time points defining time segments in R_j , $j = 1, 2$. Since

$$\begin{aligned} \Psi'(t) &= \frac{-u'(t)}{u(t)} [1 + \Psi(t)], \quad t \in R_1 \cup R_2 \\ &= 0 \quad t \in R_0 \end{aligned}$$

Therefore

$$\begin{aligned} u(t) &= \min [K_1, K_2] \quad t \in R_1 \cup R_2 \\ |1 + \Psi(t)| &> 0 \end{aligned}$$

Then $u'(t)$ bounded in $R_1 \cup R_2$ implies $\Psi'(t)$ bounded in $R_1 \cup R_2$. Thus, using a standard theorem⁽³⁾ on the order of the Fourier series, the coefficients $|d_m| < K/m^2$ where K is some number independent of m . Since the second and higher derivatives of $\Psi(t)$ are not bounded, a faster convergence rate is not implied.

Equation (14) is the main result of this paper. It is exact and holds for a very general class of input signals; that is, periodic signals of period T , and an ideal asymmetric clipper for arbitrary clipping levels $K_1 > 0$ and $-K_1 > 0$. Equation (14) then determines the complex Fourier coefficients of the output function $y(t)$ without having approximations introduced. However, in order to evaluate d_m of Eq. (14) numerically, it is necessary to determine the value of the two integrals by approximate methods which will, in turn, introduce errors in d_m and f_ℓ . The approximations can be made as accurate as desired in theory by using sophisticated computational methods to evaluate the integral. Practically, the accuracies will be limited by the capacities of the computer.

In the appendices, a number of approaches to computing the integrals in Eq. (14) are discussed for two different classes of signals. One class is typical of radio practice in that the signal is narrow band, i.e., its bandwidth is much less than any of its components. In this model it is convenient to describe the signal in terms of an envelope function modulating a carrier function. The second class of signals includes the general case of a wide-band signal having no spectral restraints. The difference between the two mathematically is that the use of envelope functions is of limited utility for a wide-band signal and so different computational techniques are required. These are discussed in more detail in Appendices B and C.

Appendix A

NARROW SINGLE SIDE-BAND TRANSMISSIONSIGNAL TYPES

Signals in physical systems are band-limited. Certain classes of signals are defined with respect to significant spectral components. A low-pass signal is one containing frequency components between zero frequency and some upper limit f_2 . A band-pass signal is defined as one whose significant frequencies lie between two frequencies f_1 and f_2 , where f_1 may be arbitrarily small but not equal to zero. (A band-pass signal has no dc component.)

The band center and bandwidth of a signal are, respectively

$$f_d = \frac{f_1 + f_2}{2}, \quad W = f_2 - f_1$$

A broad-band signal is a band-pass signal which satisfies the condition that $W \approx f_2$, while for a narrow-band signal, W is much less than f_d . Base-band speech is classified as a broad-band signal.

The above signal definitions are presented in Fig. 4.

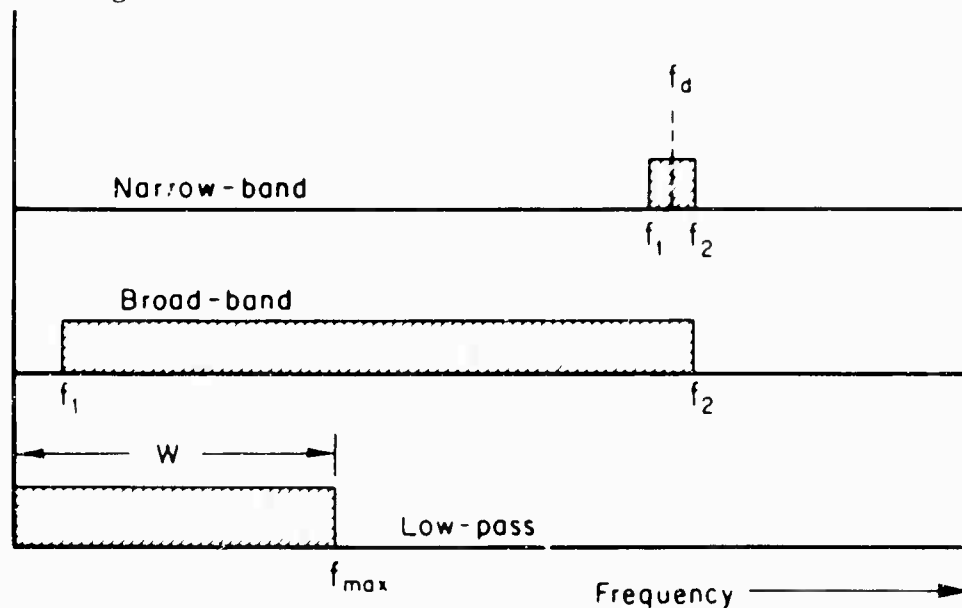


Fig. 4 — Band-limited signals

Let $s(t)$ be a narrow-band modulation signal. In order to transmit the modulation signal containing the signal intelligence, it is necessary to superimpose the signal $s(t)$ on a carrier function $h(t)$. The purpose of the carrier function is to transfer the intelligence spectrum to a frequency region more suitable for propagation. The resulting signal appears as the product⁽⁴⁾

$$u(t) = h(t) m(s(t)) \quad (\text{A-1})$$

where $h(t)$ is a function representing the carrier and m is the modulation function representing an operation on the modulation signal $s(t)$.

The development of the narrow-band signal $u(t)$ may be traced at carrier frequency ω_c from an initial low- or band-pass modulating signal $s(t)$ by inspecting Fig. 5.

Let the information signal $s(t)$ be periodic (period $T_0 = 2\pi/\omega'_0$) and band-limited with bandwidth W , where $W = N\omega'_0$. $N\omega'_0$ equals the difference between the greatest ($j_2\omega'_0$) and smallest ($j_1\omega'_0$) positive significant frequency components of $s(t)$. The carrier function is $\exp(j\omega_c t)$ which translates the spectrum of $s(t)$ by ω_c , forming the signal $v(t)$. In Fig. 5 both the positive and negative frequencies are translated, forming a double side-band signal. It is possible to pass $v(t)$ through an ideal band-pass filter, for example, which passes only the upper (lower) frequency components forming the single side-band signal $u(t)$ shown in Fig. 5-d. The signal $u(t)$ is assumed periodic; this implies that $\omega_c/\omega'_0 = a/b$ where a and b are positive integers. Further, it is assumed that $a \gg b$. If $b = 1$, then $s(t)$

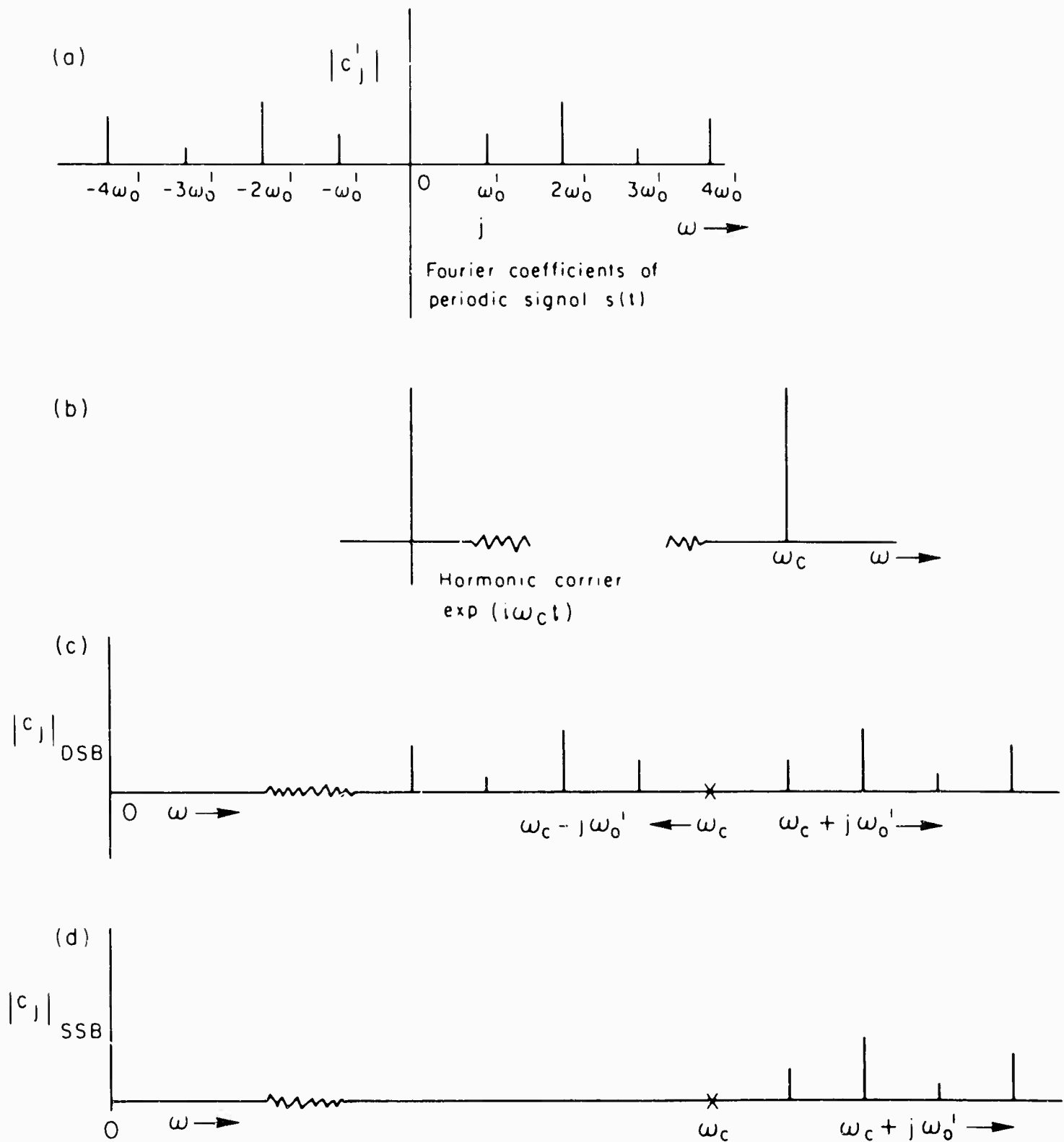


Fig. 5—Magnitude of Fourier coefficients versus frequency for (a) modulation signal; (b) carrier signal; (c) frequency translated signal, double sidebands; and (d) frequency translated signal, single sideband

periodic with period T_0 implies $u(t)$ periodic with period T_0 . If $b \neq 1$, then $s(t)$ periodic with period T_0 implies $u(t)$ periodic with period $T = bT_0$ and $\omega_0 = 2\pi/T$.

In general, ω_c and ω'_0 are not commensurate and the signal $u(t)$ will not be periodic. It is clear the values of a and b can be selected such that $|\omega_c/\omega'_0 - a/b| < \epsilon$ in this case for arbitrary small $\epsilon > 0$. The Fourier coefficients then become arbitrarily close in magnitude to the ordinates of the Fourier integral of $u(t)$ for corresponding frequencies. Resulting operations on the Fourier coefficients can then be interpreted as operations on a sampled version of the Fourier integral of $u(t)$. In order to minimize the period $T_0 b$, b should be selected as close to one as possible, thus reducing the computations required to find the values of $t \in R_1 \cup R_2$. With this understanding of the interpretation of noncommensurate ratios ω_c/ω'_0 and $b \neq 1$, it will be assumed that a and b have been selected so that negligible error occurs in using the Fourier series representation as a sampled value of the Fourier transform of $u(t)$. Thus, with no loss of generality:

- a. the signal $u(t)$ is assumed periodic with period $T = 2\pi/\omega_0$
- b. $|c_{-n}| = |c_n| = 0$, $n < a + bj_1$
 $n > a + bj_2$

Envelopes and Analytic Signals

The envelope of a time series has an intuitive meaning conjectured from elementary studies of signal modulation. In Fig. 6, it is easily "recognized" that the dotted lines are the envelope function.

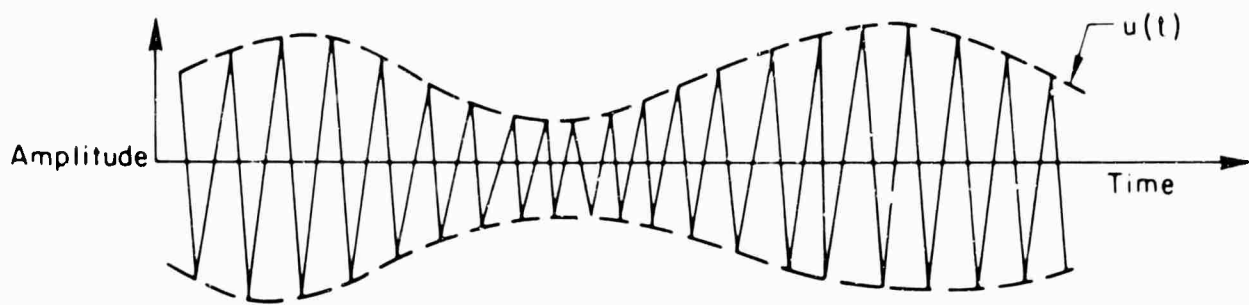


Fig.6—Modulation signal $s(t)$ superimposed on harmonic carrier

Thus, if the signal $u(t)$ is represented by

$$u(t) = A(1 + m \cos \omega_0 t) \cos \omega_c t$$

where ω_c represents the carrier frequency and ω_0 a frequency such that $\omega_c \gg \omega_0$, then the envelope function is $Am \cos \omega_0 t$.

However, for multichromatic signals, the intuitive concept of envelope soon breaks down and an envelope becomes difficult to define. Dugundji⁽⁵⁾ generalized Rice's⁽⁶⁾ formulation of the envelope of a multichromatic waveform $u(t)$ in a manner which has been found very useful in modulation theory. His generalization will be used in this paper.

Analytic Signal

Given a real valued function $u(t)$ on $-\infty < t < +\infty$, its Hilbert⁽⁷⁾ transform $\hat{u}(t)$ is defined by

$$\hat{u}(t) = \frac{1}{\pi} \int_{-\infty}^{+\infty} \frac{u(\tau)}{t - \tau} d\tau \quad (\text{A-6})$$

where the principal value of the integral is always used. All functions considered here will be assumed to have Hilbert transforms. It is easily verified that the Hilbert transform of

$$\cos(\omega t + \varphi) \text{ is } \sin(\omega t + \varphi) \quad (\text{A-7})$$

If $U(f) = \int_{-\infty}^{+\infty} u(t) \exp(-2\pi i f t) dt$ is the Fourier transform of $u(t)$, then the Fourier transform $L(f)$ of $\hat{u}(t)$ is

$$L(f) = -i U(f) \text{ sign } f \quad (\text{A-8})$$

where

$$\begin{aligned} \text{sign } z &= 1, & z > 0 \\ &= 0, & z = 0 \\ &= -1, & z < 0 \end{aligned} \quad (\text{A-9})$$

Let $u(t)$ be a real waveform; the analytic signal $z(t)$ is defined as the complex-value function

$$z(t) = u(t) + i \hat{u}(t) \quad (\text{A-10})$$

The envelope of $u(t)$ is the magnitude $|z(t)|$ of its pre-envelope.

Thus, if a signal $u(t)$ is given by

$$u(t) = \sum_n d_n \cos(\omega_n t + \varphi_n) \quad (\text{A-11})$$

forming the pre-envelope of $u(t)$ gives

$$z(t) = \sum_n d_n \cos(\omega_n t + \varphi_n) + i \sum_n \sin(\omega_n t + \varphi_n) \quad (\text{A-12})$$

Before proceeding, the formulas for the envelope and pre-envelope must be modified for periodic signals.

The Fourier series⁽⁸⁾ in complex form of $s(x)$ is defined as

$$s(x) = \sum_{k=-\infty}^{+\infty} c'_k e^{ikx} \quad (\text{A-13})$$

and the conjugate series obtained by replacing c'_k by $c'_k = -i c'_k \text{sign } k$

$$\bar{s}(x) = -i \sum_{k=-\infty}^{+\infty} c'_k \text{sign } k e^{ikx} \quad (\text{A-14})$$

for $s(x)$, $0 \leq x < 2\pi$, $x = v_0 t$.

The function $\bar{s}(x)$ is equivalent to the Hilbert transform $\hat{s}(x)$ which must be used for periodic functions.

The transform relationship may be expressed as

$$\bar{s}(x) = \lim_{h \rightarrow 0} -\frac{1}{\pi} \int_{-h}^h \frac{s(x+v) - s(x-v)}{2 \tan \frac{1}{2}v} dv \quad (\text{A-15})$$

or alternately

$$\bar{s}(x) = \frac{-1}{\pi} \int_0^{\infty} \frac{s(x+v) - s(x-v)}{v} dv \quad (\text{A-16})$$

Dugundji⁽⁵⁾ establishes the following lemma:

Let $u(t)$ be a waveform having frequency spectrum in the bands $f_c - \frac{1}{2}W$ and $f_c + \frac{1}{2}W$. Then the square of the envelope magnitude is frequency limited to $f \leq W$. Dugundji remarks that "one may not conclude that the envelope itself is band-limited, indeed there seems to be no physical reason that it should be so." The band-limited property of the square magnitude of the envelope is the basis for the interest in the envelope function $|z(t)|$.

Clipping is performed on the signal $u(t)$ of Eq. (A-1) before transmission. The fine structure imposed on $s(t)$ by the carrier function $h(t)$ (see Fig. 6) makes it much more difficult to compute the regions R_1 and R_2 required to evaluate the integrals I_1 and I_2 of Eq. (14). It is easier to determine the regions R_j of the envelope in Fig. 6 than of each of the individual cycles of the fine structure. Thus, by computing $|z(t)|^2$, a function of considerably less fine structure can be considered.

The regions R_1 and R_2 may be determined for $|z(t)|^2$, as follows: Let $X = \min \{K_2^2, K_1^2\}$.

Then the region $R \in |z(t)|^2 > X$ can be obtained by any one of a number of methods. For example

- a. Plot $|z(t)|^2$ versus (t) and read from the intersections of the curve $|z(t)|^2$ with the line $z^2 = X$.
- b. Let $z^2 = x(t)$. Compute z^2 at sufficiently close intervals so that every significant peak of z^2 is sampled.

From the sampling theorem $\Delta\tau = \frac{1}{2W}$, it should be sufficient to determine z^2 uniquely at each point. However, if, for example, there is no concern with peaks of widths less than Δt , this may be

relaxed. In this case, a sampling interval $\Delta t/2$ would be sufficient to locate approximately the regions of significant peaks.

Once the approximate location of t_1 , for example, is obtained by finding values of t_1' , t_1'' such that

$$x(t_1') < X < x(t_1'') \quad (\text{A-17})$$

Then, interpolation formulas may be used to obtain more accurate values of t_1 , e.g.

$$t_1 = t_1' - \frac{x(t_1') - X}{\frac{d}{dt} x(t_1')}, \quad \frac{d}{dt} x(t_1') \approx \frac{x(t_1) - x(t_1')}{t_1 - t_1'} \quad (\text{A-18})$$

can be solved iteratively.

The degree of accuracy of t_1 required is about one-fourth of a cycle of the carrier frequency ω_c . The same comments on accuracy are true for graphical solutions.

- c. If $x(t)$ is of sufficiently simple analytic form, divide $x(t)$ into nonincreasing and nondecreasing sections. In each section note if $\max x(t) \leq X$. In the sections satisfying the last requirement, invert the function to determine the set

$$\{t\} \in x^{-1}(t) = X.$$

If these operations can be performed analytically, then the required accuracy is limited only by the computational effort required to compute $x^{-1}(t)$.

- d. If the maxima of the envelopes can be determined analytically, then considerable computation effort can be saved by method (b) only in the vicinity of the maxima exceeding X and at the $t = 0$ to the time of the first maxima, and from the time of the last maxima to time T .

The above techniques will then define the regions where the envelope $z(t)$ exceeds $X^{\frac{1}{2}}$. To define the regions where the transmitted signal $u(t)$ lies in the regions R_1 and R_2 , the following procedure should be undertaken.

Considering the case of a single side-band amplitude modulated signal, ⁽⁴⁾ Eq. (A-1) can be written as

$$m(t) = s(t) + i \hat{s}(t) \quad (\text{A-19})$$

$$\begin{aligned} z(t) = & [s(t) \cos \omega_c t - \hat{s}(t) \sin \omega_c t \\ & + i [s(t) \sin \omega_c t + \hat{s}(t) \cos \omega_c t]] \end{aligned} \quad (\text{A-20})$$

$$\begin{aligned} \text{from which } z(t) = & [s^2(t) + \hat{s}^2(t)]^{\frac{1}{2}}, \quad \omega_c > 0 \\ = & [s^2(t) + \hat{s}^2(t)]^{\frac{1}{2}} \quad \text{for periodic signals} \end{aligned} \quad (\text{A-21})$$

If the signal to be recovered is $s(t)$ ($\hat{s}(t)$), then the transmitted signal is the real (imaginary) part of $z(t)$. The real part of $z(t)$ can be written for periodic signals as

$$u(t) = |z(t)| \sin \left[\omega_c t - \tan^{-1} \frac{s(t)}{\hat{s}(t)} \right] \quad (\text{A-22})$$

The maxima of $|u(t)|$ occur in the neighborhood of \tilde{t}_n where \tilde{t}_n is the solution of the equations

$$\arctan t - \tan^{-1} s(t)/\bar{s}(t) = \frac{(2n+1)\pi}{2}, \quad n = 0, 1, 2, \dots, \tilde{t}_n \in R_1 \cup R_2 \quad (\text{A-23})$$

Eq. (A-23) can be solved iteratively as follows

$$\begin{aligned} \text{Set } t_n^{(j)} &= \frac{\frac{(2n+1)\pi}{2} + \tan^{-1} s(t_n^{(j-1)})/\bar{s}(t_n^{(j-1)})}{t_c} \\ t_n^{(0)} &= \frac{(2n+1)\pi}{2} t_c \\ \tilde{t}_n &= \lim_j t_n^{(j)} \end{aligned} \quad (\text{A-24})$$

Where the values of n are selected such that $t_n^{(0)} \in R_1 \cup R_2$. If $|z(t)|$ has been programmed for a computer, then values of $s(t)$ and $\bar{s}(t)$ are easily available for the iterative solution of Eq. (A-24).

For graphical computations, graphs of $s(t)$ and $\bar{s}(t)$ are required, and Eq. (A-24) can then be computed from graphical readings. The exact location of the \tilde{t}_n is not critical if there are many peaks of the fine structure of $u(t)$ in a peak of the envelope $|z(t)|$ as shown in Fig. 7.

Having found the value \tilde{t}_n for a specific spike in R_1 , then $\Delta t_n = \frac{\pi}{\omega_c}$ may be added to estimate the corresponding maxima point for the adjacent carrier spike in R_2 . If the phase correction does not vary rapidly over a number of carrier spikes, a small correction can be used for subsequent \tilde{t}_n as follows.

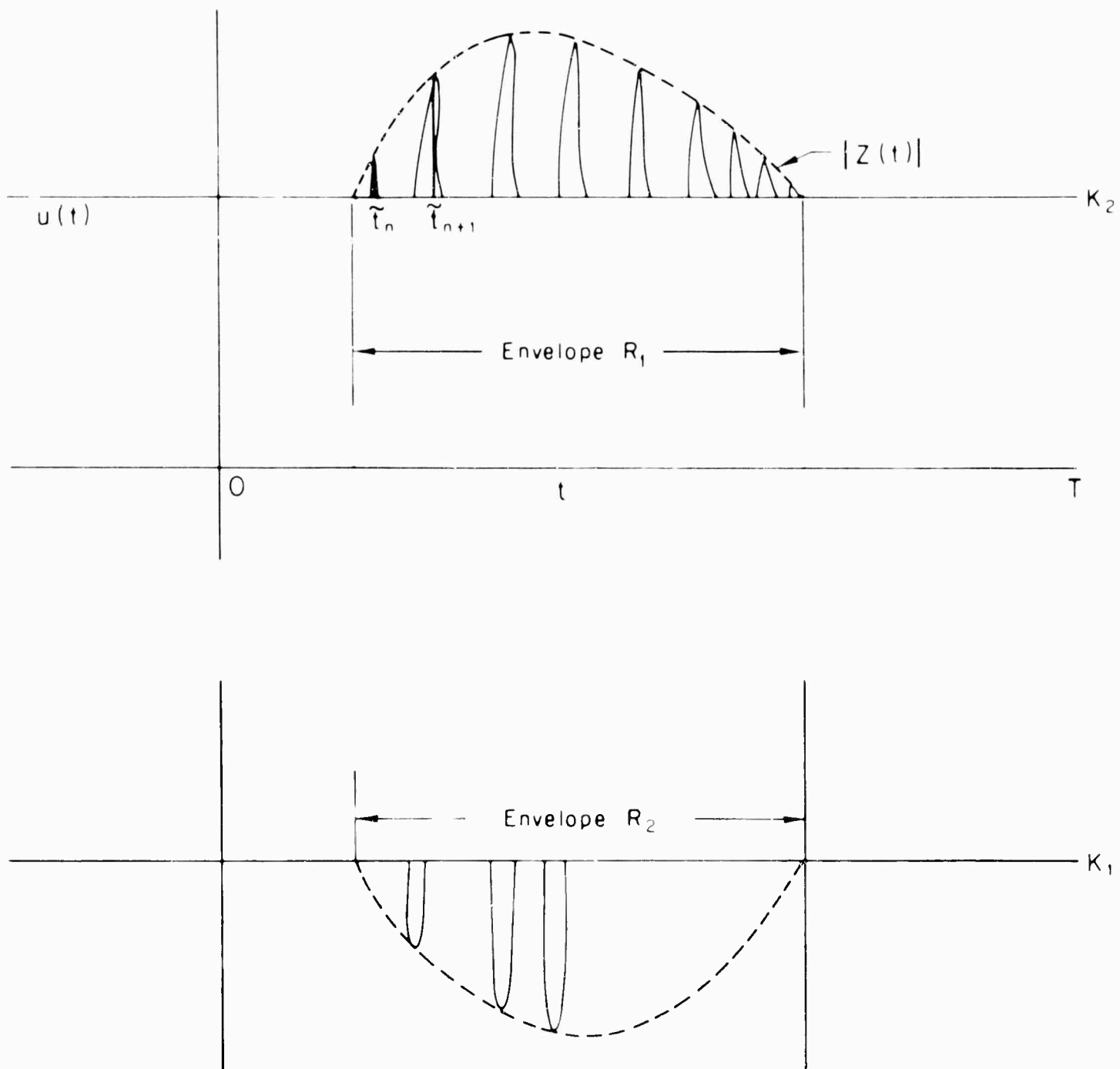


Fig.7—Typical display of clipped peaks of transmitted signal for $t \in R_1$ and R_2 showing fine structure of carrier function

Let \tilde{t}_n be the abscissa of the maxima point of the first carrier peak in R_1 of Fig. 7. Then an initial estimate for t_{n+1} , the next abscissa, is given by

$$t_{n+1}^{(0)} = \tilde{t}_n + 2\pi/\omega_c$$

provided $t_{n+1}^{(0)} \in R_1$. The iterative Eq. (A-24) may be used to refine estimates of \tilde{t}_{n+1} .

EVALUATING THE INTEGRALS I_1 AND I_2

Assuming that the sequence of values $\{\tilde{t}_n, |z(\tilde{t}_n)|\}$ in $R_1 \cup R_2$ defining the position and values of the carrier peaks has been obtained, $I_1(m)$ and $I_2(m)$ may be evaluated as follows.

Assume that $z(t)$ is essentially constant and equal to $z(\tilde{t}_n)$ over a cycle of the carrier frequency. For $\tilde{t}_n \in R_1$, \tilde{t}_n can be expressed in the neighborhood of (within one cycle of ω_c)

$$u(t) = |z(\tilde{t}_n)| \cos(\omega_c(\tilde{t}_n - t)) \quad (\text{A-25})$$

For $\tilde{t}_n \in R_1$

$$u(t) = |z(\tilde{t}_n)| \cos(\pi + \omega_c(\tilde{t}_n - t)). \quad (\text{A-26})$$

The solution to the equations

$$u(t_n^*) = K_1 \quad (\text{A-27})$$

is

$$|\tilde{t}_n - t_n^*| = \frac{1}{\omega_c} \cos^{-1} [K_1/|z(\tilde{t}_n)|] \quad (\text{A-28})$$

Let

$$\Delta t_n = \tilde{t}_n - t_n^* \quad (\text{A-29})$$

$I_1(m)$ can be expressed as

$$I_1(m) = \frac{-1}{T} \sum_{\tilde{t}_n \in R_1} e(-im\omega_0 \tilde{t}_n) \int_{-t_n}^{+t_n} \frac{|z(t_n)| \cos \omega_c \tau - K_1}{|z(\tilde{t}_n)| \cos \omega_c \tau} c(im\omega_0 \tau) d\tau \quad (\text{A-30})$$

If the Fourier coefficients d_m of the clipping function $c(t)$ drop off rapidly as (m^{-2}) , only values of $m \leq \omega_c/\omega_0$ are of concern.

Therefore

$$I_1(m) = \frac{-2}{T} \sum_{\tilde{t}_n \in R_1} e(-im\omega_0 \tilde{t}_n) \int_0^{\Delta t_n} \frac{|z(\tilde{t}_n)| \cos \omega_c \tau - K_1}{|z(\tilde{t}_n)| \cos \omega_c \tau} d\tau \quad (\text{A-31})$$

The integral in Eq. (A-31) can be evaluated (Dwight, Tables of Integrals, #442.10)

$$I_j(m) = \frac{-2}{T} \sum_{\substack{\tilde{t}_n \in R_j \\ j=1,2}} e(-im\omega_0 \tilde{t}_n) \left[\Delta t_n + \frac{(-1)^j K_j}{|z(\tilde{t}_n)|} \frac{1}{2\omega_c} \log \frac{1 + \sin \omega_c \Delta t_n}{1 - \sin \omega_c \Delta t_n} \right] \quad (\text{A-32})$$

For light limiting $\omega_c \Delta t_n \ll 1$, then to first order in $\omega_c \Delta t_n$

Eq. (A-32) reduces to

$$I_j(m) = \frac{-2}{T} \sum_{\tilde{t}_n \in R_j} e(-im\omega_0 \tilde{t}_n) \left[\Delta t_n \left(1 + \frac{(-1)^j K_j}{|z(\tilde{t}_n)|} \right) \right] \quad j=1,2 \quad (\text{A-33})$$

where $K_1 \neq 0$, $K_2 \neq 0$

Equation (A-33) or (A-32) combined with Eq (14) gives the coefficients d_m necessary to determine the corrections of the input Fourier coefficients.

Appendix B

BROAD-BAND SIGNALS

In this appendix the modulation signal $s(t)$ is taken to be broad band, say of the order of the carrier frequency (see Fig. 4). In this case the envelope function does not provide any advantages since its fine structure is as complicated as the fine structure of the transmitter signal $u(t)$. Further, because of the fine structure of $u(t)$, a digital computation of $u(t)$ to determine the regions $t \in R_1 \cup R_2$ may involve excessive calculations.

Thus, it is expedient to use analog computations to obtain the coefficients d_m of the limit time function $c(t)$. Then, the specific Fourier components of the output signal of interest can be computed, using Eq. (1). In general, the analog computations are efficient in determining the regions $t \in R_1 \cup R_2$. When these regions have been determined, the integrals $I_j(m)$ can be determined either by analog methods or, if great accuracy is required, by numerical methods; i.e., by computing $u(t)$ in a fine mesh in the region of the peaks of $u(t)$ such that $t \in R_1 \cup R_2$ and performing the integrations of $I_j(m)$ given by Eqs. (15) and (16) numerically.

Figure 8 presents a completely analog solution for the Fourier coefficients d_m . The signal is generated at some arbitrary time t , taken to be zero. The signal is passed through two circuits. The upper circuit compares $u_1(t)$ with K_1 . If $u(t) > K_1$, a gate permits the difference $(u(t) - K_1)$ to be transmitted as a voltage versus time. Another gate permits the inverse of $u(t)$ to pass on a separate channel. If the test fails, no voltage is transmitted in either channel. The two

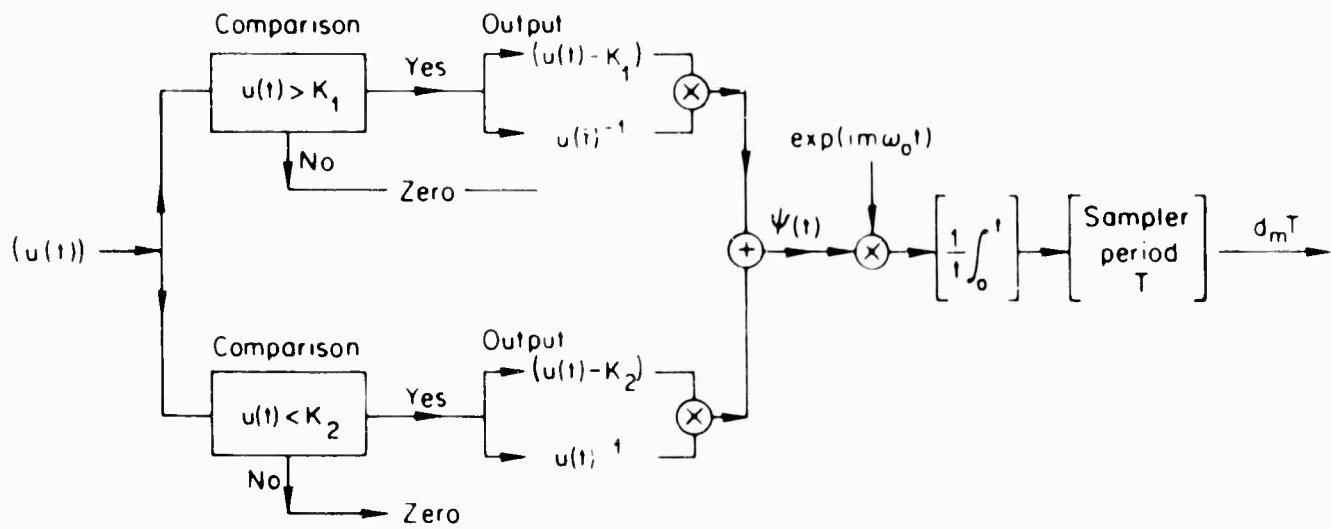


Fig.8—Analog solution for the Fourier coefficients d_m of the limit function $c(t)$

channel outputs are multiplied and added to a similar channel based on the test $u(t) = K_2$. The result of the addition is the function $\psi(t)$ shown in Fig. 3. The $\psi(t)$ channel is multiplied by an input channel $e^{-1m\omega_0 t}$. All times must be synchronized to the same origin. The product is integrated and divided by the total time from zero. The output of the integrator sampled at times $T, 2T, 3T, \dots$ will be $d \cdot T$.

This solution has the advantages of speed and simplicity but is limited in accuracy by the analog nature of the calculation.

A hybrid analog-digital technique is shown in Fig. 9. The analog computer consists of two channels. In the upper channel if $u(t) > K_1$, a +1 is the output; if $u(t) \leq K_1$, zero is the output. The square pulse corresponding to $t \in R_1$ is then fed into a derivative circuit whose output is the positive spike for the leading edge of the pulse and a negative spike for the tail edge of the pulse. A counter counts the number of cycles from time zero to the spikes and the output is the set of time intervals ϵR_1 . The lower channel operates in a similar manner. These time intervals can be used as the input to a digital program as previously described. This hybrid technique has the advantage of using the best of both systems. The analog solution for the interval $(t_i, t_j) \in R_1 \cup R_2$ is obtained much more quickly and easily than the digital solution for these intervals. However, there is no loss of accuracy since the digital program can interpolate for greater accuracy and perform the remaining numerical integrations to a very high degree of precision.

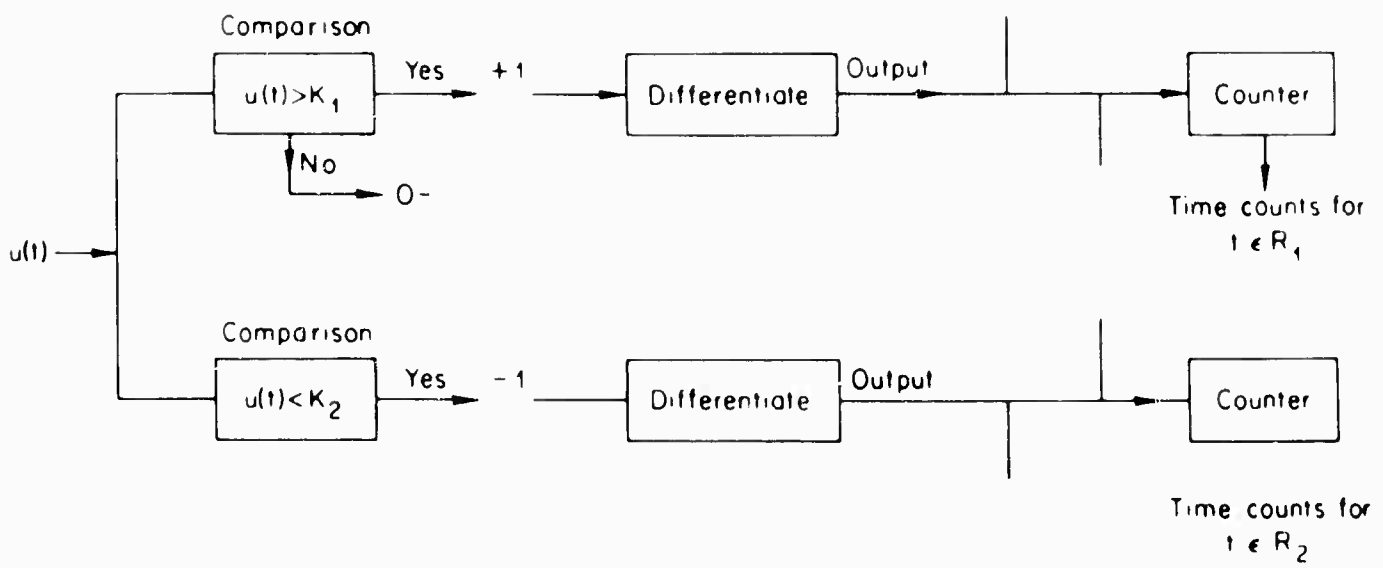


Fig.9—Analog solution for times $t \in R_1 \cup R_2$

This technique may even have advantages in the narrow-band case for determining the locations of \hat{f}_n and \hat{t}_n , and then proceeding with the computations of Eq. (A-31) or (A-33).

It will require some actual computing experience to determine which of the methods is most suitable for determining the required Fourier coefficients of the various classes of modulation signals.

Appendix C

SENSITIVITY OF THE VALUE OF INTEGRALS $I_1(\omega)$ TO CARRIER FREQUENCY ω_c

It will be shown that if the envelope function is a slowly varying function of time relative to the carrier frequency ω_c , changing the carrier frequency will have little effect as long as $z(t)$ is essentially constant. This will be demonstrated by showing that in the limit for constant envelope, the integrals $I_1(0)$ and $I_2(0)$ are independent of carrier frequency.

Define

$$u_n(x) = z(x) \sin nx$$

Let $z(x) = 1$

Define

$$J_n = \int_{x \in R_1} \frac{(u_n(x) - K_1)}{u_n(x)} dx$$

where for convenience $x = \omega_c t$, $0 \leq x \leq 2\pi$

and $x \in R_1$ is the set of points such that

$$u_n(x) \geq K_1, \quad 0 < K_1 < 1$$

Let $n = 1$, then $x \in R_1$ is defined by the set of points

$$-\hat{x} + \frac{\pi}{2} \leq x \leq \hat{x} + \frac{\pi}{2}$$

where $\hat{x} = \sin^{-1} K_1$

$$0 < \hat{x} < \frac{\pi}{2}$$

$$J_1 = \int_{\frac{\pi}{2} - \hat{x}}^{\frac{\pi}{2} + \hat{x}} \frac{(\sin x - K_1)}{(\sin x)} dx$$

Let $x = \frac{\pi}{2} - v$, then it is easily shown that

$$J_1 = - \int_0^{\hat{x}} \frac{(\cos(v) - K_1)}{\cos(v)} dv$$

J_1 has the same form as $J_1(0)$ (except for sign) with $z(t) = 1$

Consider the value of J_n

$$J_n = \int_{x \in R_1} \frac{(\sin nx - K_1)}{\sin nx} dx$$

It is easily shown that J_n consists of n integrals of equal value. A typical integral is, for example, integrated over the first peak, e.g.,

$$\frac{\pi}{2n} - \frac{1}{n} \hat{x} \leq x \leq \frac{\pi}{2n} + \frac{1}{n} \hat{x}$$

Therefore

$$J_n = n \cdot \int_{\frac{\pi}{2n} - \frac{1}{n} \hat{x}}^{\frac{\pi}{2n} + \frac{1}{n} \hat{x}} \frac{(\sin nx - K_1)}{\sin nx} dx$$

By substituting $nx = \pi/2 - v$, it is easily shown that

$$J_n = J_1$$

Thus, the integral J_n which is equivalent to I_1 , is independent of n . The parameter n plays the role of the carrier frequency and for constant envelope $z(t)$, the integrals $I_1(0)$ and $I_2(0)$ will be independent of the carrier frequency. For slowly varying $z(t)$ it can be assumed that I_1 and I_2 will be insensitive to changes in carrier frequency which are large compared to the bandwidth of $z(t)$.²

REFERENCES

1. Shyne, N.A., Speech-signal Processing and Applications to Single Sideband, Electronics Research Laboratory, Montana State College, Final Report AFRL-62-64, March 1962.
2. Wathen-Dunn, W., and D.W. Lipek, "On the Power Gained by Clipping Speech in the Audio Band," JASA, Vol. 30, 1957, p. 36.
3. Carslaw, H., Introduction to the Theory of Fourier Series and Integrals, Third Edition, Dover Publications, New York, 1930.
4. Bedrosian, F., The Analytical Signal Representation of Modulated Waveforms, The RAND Corporation, RM-3089-1-1K, September 1962.
5. DuRandji, J., "Envelopes and Pre-envelopes of Real Waveforms," IRE Trans. Info. Theory, Vol. 11-3, March 1965, pp. 33-9.
6. Rice, S.O., "Mathematical Analysis of Random Noise," BSIJ, Vol. 23, 1944, p. 1.
7. Titchmarsh, E.C., Introduction to the Theory of Fourier Integrals, Oxford University Press, New York, 1937.
8. Zygmund, Antoni, Trigonometrical Series, Dover Publications, New York, 1955.

ADDITIONAL REFERENCES

- Kahn, L.R., "The Use of Speech Clipping in Single Side Band Communication Systems", Proc. IRE, Vol. 45, No. 8, August 1957, p. 1148.
- Martin D.W., "Uniform Speech Clipping in a Uniform Signal-to-Noise Spectrum Ratio," JASA, Vol. 22, 1951, p. 614.
- Smith, W.W., "Premodulation Speech Clipping and Filtering," QST, Vol. 30, 1946, p. 46.